Supercooled Liquid Water and Ice Crystal Distributions Within Sierra Nevada Winter Storms

MARK F. HEGGLI AND LARRY VARDIMAN[1]

U.S. Bureau of Reclamation, Auburn, CA 95603

RONALD E. STEWART

Atmospheric Environment Service, Downsview, Ontario, Canada M3H 5T4

ARLEN HUGGINS

Electronic Techniques Inc., Auburn, CA 95603

(Manuscript received 11 March 1983, in final form 1 August 1983)

ABSTRACT

Cloud physics data measured by aircraft during two successive winter field seasons (1978–79 and 1979–80) of the Sierra Cooperative Pilot Project operating over the Sierra Nevada Range have been examined in order to determine the distributions of supercooled liquid water and ice crystals. Results indicate that convective clouds provide the greatest likelihood of significant supercooled water. The Sierra barrier appears to optimize these conditions 40 to 90 km upwind of the crest within pockets of horizontal extent up to 64 km, although these conditions were greatly reduced at temperatures less than −10°C. The dominance of liquid water content over ice crystal concentration was maximized 7–10 h after the 700 mb trough passage. Area-wide and banded clouds, which make up the remaining precipitation events, showed only small amounts of supercooled water and general abundance of ice crystals. The largest liquid water contents were observed at the greatest temperatures, usually 0° to −5°C. Such climatological information suggests that a weather modification program to enhance snowfall should concentrate primarily on the convective clouds.

1. Introduction

The potential for enhancing snowfall in winter orographic clouds is usually associated with the presence of supercooled liquid water in an ice-deficient environment. Because direct measurement of liquid water content (LWC) and ice crystal concentration (ICC) historically has been difficult, many estimates of seeding potential have been made by indirect means such as cloud top temperature, condensate supply rates, etc. However, as aircraft instrumentation has improved, direct measurement of LWC and ICC has become more prevalent.

Some of the more recent direct measurements of LWC and ICC in winter orographic clouds have been made by Hobbs (1975a, 1975b), Hobbs and Radke (1975), Lamb *et al.* (1976), Marwitz (1980), Cooper and Saunders (1980), Cooper and Marwitz (1980), and Marwitz and Stewart (1981). These measurements are leading to the realization that ideal conditions for seeding are more limited than previous estimates had indicated, because of lower concentrations and frequencies of LWC and higher concentrations and frequencies of ICC.

The Sierra Cooperative Pilot Project (SCPP), administered by the Bureau of Reclamation, has made extensive airborne measurements of LWC and ICC over the central Sierra Nevada range. The SCPP with the project area shown in Fig. 1, is a research program directed towards determining the feasibility of weather modification as a means to supplement the regional water supply in central California and western Nevada. This article reports on these observations of supercooled liquid water and ice crystals within central Sierra storms. Suggestions are made in regards to possible seeding potential within different cloud types.

2. Instrumentation platforms

A collection of meteorological instrumentation was used to study the Sierra Nevada winter storms. The equipment was deployed over the American and Tahoe–Truckee river basins in California and Nevada. Data were obtained during the 1978–79 and 1979–80 field seasons which coincided with the winter months of January through March. The two primary data sources used in this study were the cloud physics aircraft and weather radar.

[1] Current affiliation: Christian Heritage College, San Diego, CA.

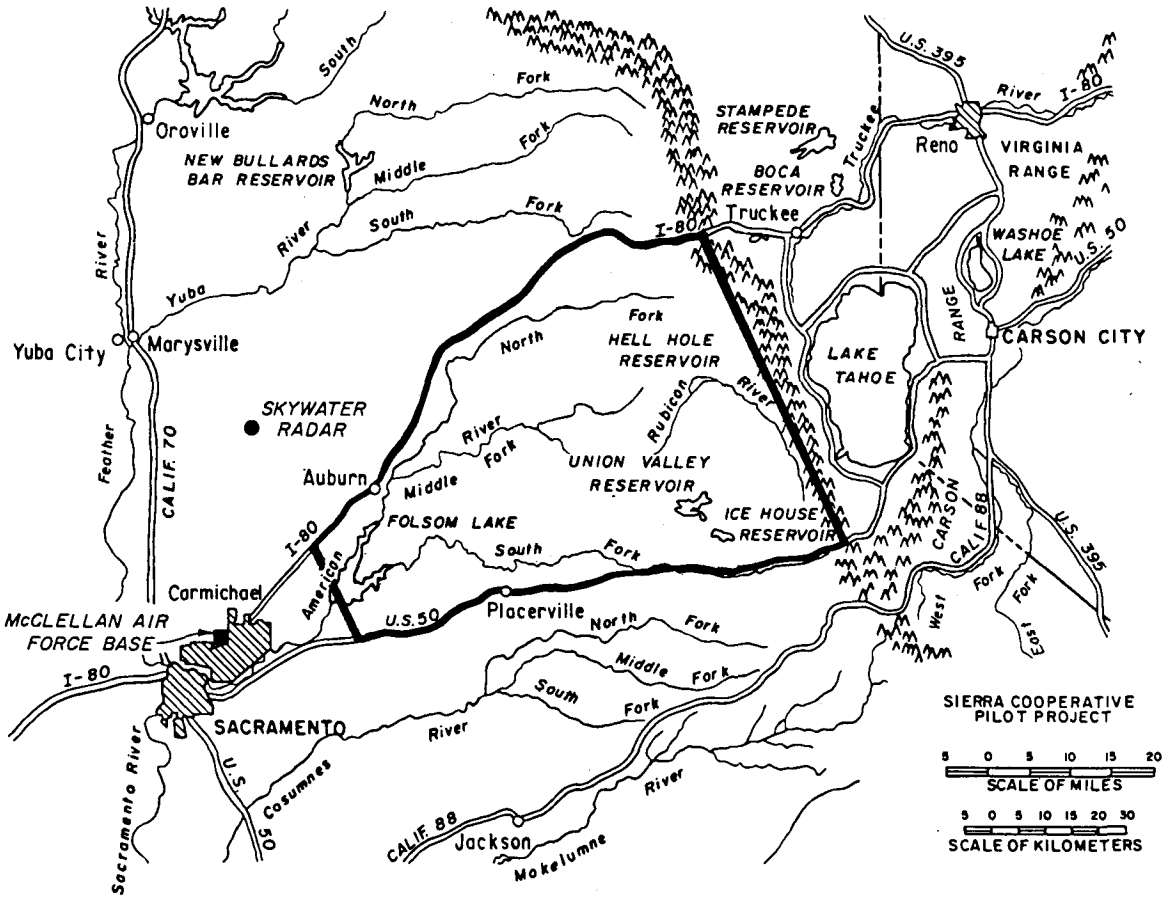

FIG. 1. The Sierra Cooperative Pilot Project study area (outlined).

a. Airborne data acquisition techniques

The University of Wyoming operated a Beechcraft Super King Air 200 aircraft during the winters of 1978–79 and 1979–80. Two measurement systems were used to determine the LWC. A forward scattering spectrometer probe (FSSP), described by Knollenberg (1976), provided a continuous measurement of the cloud droplet spectrum from which the LWC was calculated. The FSSP measured droplet diameter from 2 to 30 μm in 2 μm intervals. A Johnson-Williams (JW) hot wire device provided an independent means of determining LWC. The measurement aspects of these two instruments were studied by Marwitz and Stewart (1981). In regions where the JW-derived LWC was less than 0.1 g m^{-3} the FSSP LWC was used, otherwise the JW was the primary device. The JW was shown by Knollenberg (1972) to be restricted in regions of low LWC. In addition, Strapp and Schemenauer (1982) also discussed measurement dependency of several JW devices with airspeed, temperature, and the amount of LWC. Ice crystal measurements were made with a 2D-C optical array probe which is described by Knollenberg (1976). The 2D-C recorded particle diameter, shape, and concentration in the range of 25 to 800 μm at 25 μm intervals. Processing software and other aspects of the King Air instrumentation have been described in detail by Cooper (1978).

b. Skywater radar

A 5.4 cm wavelength SKYWATER radar was located near Sheridan, California. The radar range was 140 km. Programmed volume scans were made at 5 min intervals. The radar was capable of detecting minimum equivalent reflectivities of 6.5 dB(Z) at 50 km and 14.5 dB(Z) at 125 km. Additional technical information regarding the SKYWATER radar can be found in Schroeder and Klazura (1978).

3. Stratification of data

Digital radar data, collected in support of aircraft operations, were stratified by seven precipitation echo types (PET) as described in Table 1 and shown in Fig. 2. A PET was classified from plan position indicator (PPI) scans.

Analysis of SCPP rawinsonde data, which were taken near Sheridan, California, has shown that the echo

TABLE 1. Description of seven precipitation echo types.

Precipitation echo type	Description
Orographic (O)	An orographic echo (Fig. 2a) is a reasonably uniform echo tied to the higher topography. The bright band is often observed in this echo, as are generating cells and varying degrees of embedded convection.
Area-wide (AW)	This echo (Fig. 2b) is so named because it frequently covers the entire radar scope and is of much larger scale than the other types. It is uniform in nature and is not tied to the higher topography. The bright band is nearly always observed in this PET.
Embedded band (EB)	This feature (Fig. 2f) is commonly observed in AW or O echoes as elongated regions of enhanced reflectivity which generally move west to east through weaker surrounding echo. Motion is usually normal to the major axis of the band. Reflectivities can reach 50 dB(Z) in the bright band and average rainfall rates are higher than these from any other PET.
Major band (MB)	The major band (Fig. 2g) is a well organized mesoscale feature observed as an elongated area of reflectivity with either strong reflectivity gradients or of sufficiently large scale to be easily identified. It generally moves normal to its major axis. The circulations associated with a band often suppress radar echoes ahead and behind it.
Convective train (CT)	A convective train (Fig. 2c) is a nonuniform echo organized in a line with cellular echoes tending to develop from a single generating point. The point may or may not be fixed. Individual cells within CT tend to propagate downwind as they grow along a nearly stationary line. This echo pattern is often found only on the mountain barrier, but is sometimes observed to exist across the entire Sacramento Valley and onto the barrier.
Cellular structure (>50% coverage, C2)	This is a pattern of convective elements that exist as individual cells or clusters of cells (Fig. 2d) and cover more than one half of an area. Unlike the other types, coverage refers to the region of convective activity (as defined by radar echoes) and not the entire American River Basin. C2 often covers an area similar to orographic echo but is less uniform in appearance.
Cellular structure (≤50% coverage, C1)	This echo type is similar to C2 except coverage must be less than one half of the region where convection is occurring (Fig. 2e).

types were associated with significantly different lapse rates of equivalent potential temperature (θ_e). Fig. 3 presents the mean lapse rates of θ_e for each PET. The profiles generally show increasing convective instability from right to left as indicated by data taken from 1976–77 through 1979–80.

The various echo types have been observed in a variety of synoptic conditions, but a distinct sequence of echo types is often observed in well organized cyclonic storms with their associated and well defined 700 mb trough passages. The occurrence of AW echoes was almost entirely pretrough with a peak 5–6 h ahead of trough passage. Major bands were widely distributed before and after trough passage with a major peak 2 h ahead of the trough and minor peaks 1 and 3 h behind the trough. The distribution of embedded bands was centered on trough passage. The C1, C2, and CT echo types were post-trough phenomena with peaks at 7, 4.5, and 5.5, respectively, behind the trough. Orographic echoes occurred mostly post-trough with a broad distribution peak 2 h after passage.

Because the amount of aircraft data available for each PET was limited, it was decided to combine PETs into three major categories. The three combinations are shown in Table 2, with the respective number of days that each type and combinations were flown. Table 2 also shows the percentage frequency of occurrence of each echo type derived from radar from five winter field seasons, from 1976–77 to 1981–82, not including 1980–81 when there were no operations.

The area-wide combination (O, AW, WB) represents a relatively stable subset of the seven echo types. The banded subset (MB, CT) is made up of two distinct echo features, which were combined based on their frequent simultaneous occurrence. The CT type is very unstable and the MB is a mixture of stable and unstable environs. The cellular combination (C1, C2) represents the unstable cumulus convective elements.

4. The LWC/ICC ratio

Magnitudes and distributions of LWC and ICC in clouds can be used to help estimate opportunities for augmenting precipitation at the ground. Many other variables such as wind velocity and shear, cloud lifetimes, terrain influences, and precipitation trajectories need to be considered when making a complete assessment of seeding opportunities. However, if the candidate clouds have insufficient liquid water content and an overabundance of ice crystals initially, the remaining considerations are academic.

We believe the LWC/ICC ratio is a good measure of the microphysical potential for enhancing precipitation. It is possible that when our measure of seedability looks adequate in a given situation, other factors may still negate attempts to increase precipitation at the ground. We believe that these factors can be evaluated independently at later steps in the precipitation process.

It is understood qualitatively by those working in cloud physics and weather modification that when a cloud has a large LWC it is most likely to respond to

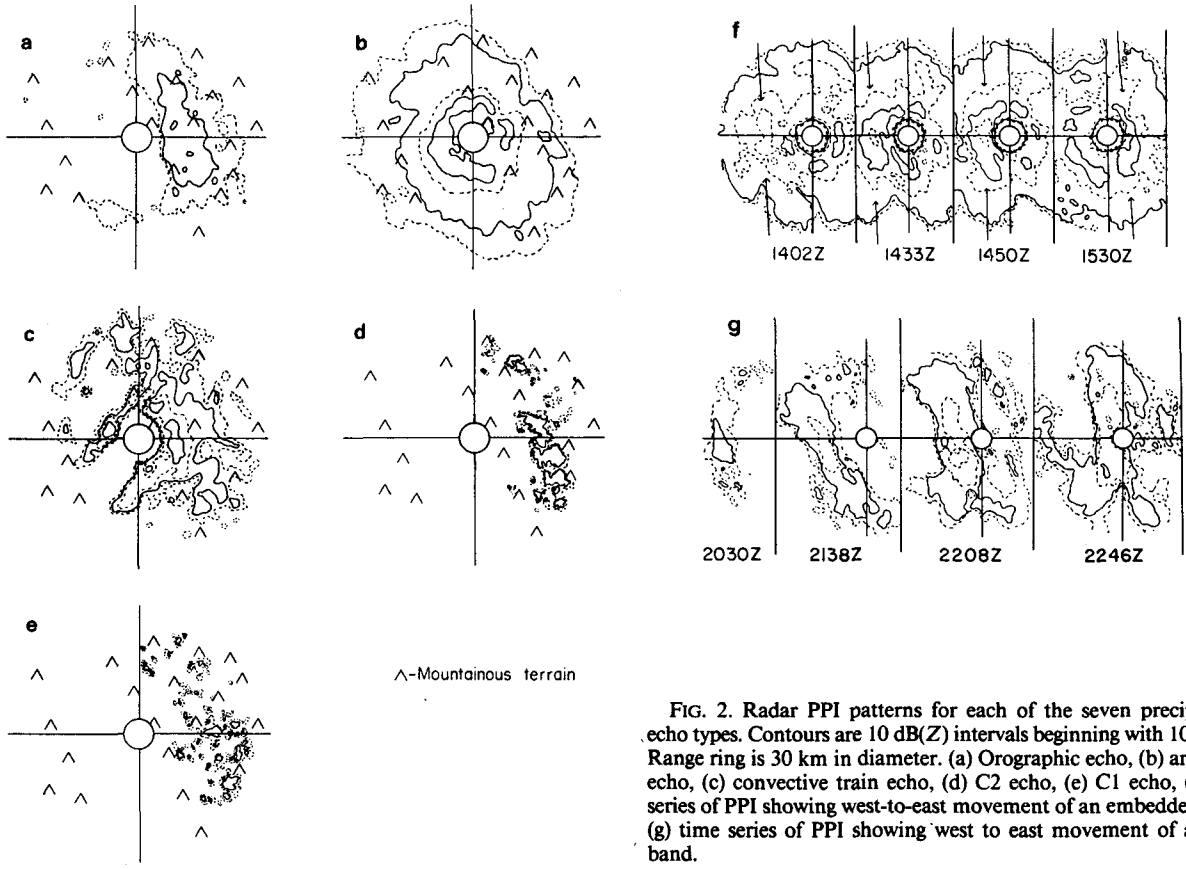

FIG. 2. Radar PPI patterns for each of the seven precipitation echo types. Contours are 10 dB(Z) intervals beginning with 10 dB(Z). Range ring is 30 km in diameter. (a) Orographic echo, (b) area-wide echo, (c) convective train echo, (d) C2 echo, (e) C1 echo, (f) time series of PPI showing west-to-east movement of an embedded band, (g) time series of PPI showing west to east movement of a major band.

seeding. Likewise, when a cloud has a greater ICC it is less likely to respond to seeding, or at least respond observably (see Cooper and Marwitz, 1980; Hobbs, 1975b; Marwitz and Stewart, 1981). Since cold-cloud seeding is an attempt to introduce ice crystals into a cloud and convert liquid water to ice crystals, we believe that a simultaneous measure of these two variables is necessary to develop a quantitative measure of seed-

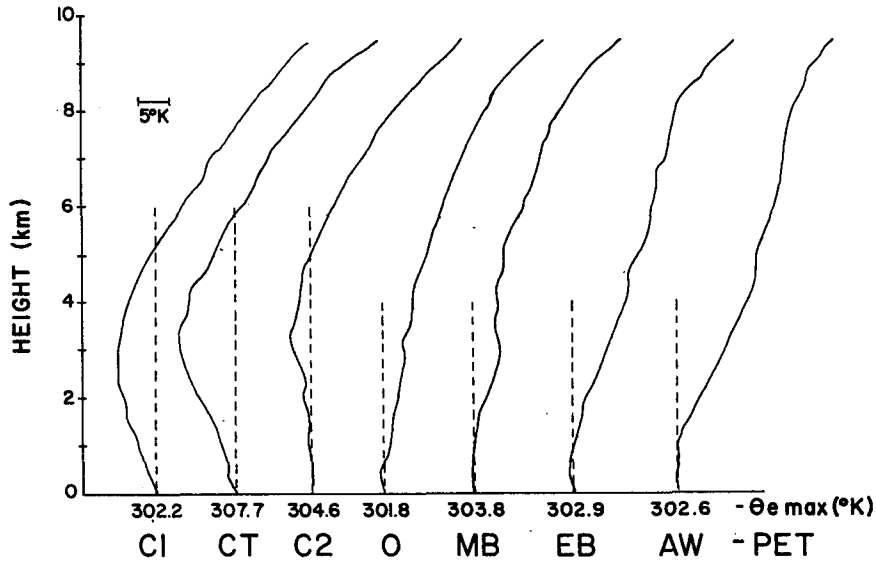

FIG. 3. Mean lapse rates of equivalent potential temperature for the precipitation echo types.

TABLE 2. Number of days each echo type and combination were flown for the two-year period of study (1978–79, 1979–80) and the percentage frequency of occurrence of the echo types from five winter field seasons (1976–77 to 1981–82, not including 1980–81 when there were no aircraft or radar operations).

	Area-wide			Banded		Cellular	
	AW	O	EB	MB	CT	C1	C2
1978–79	3	6	5	3	1	10	6
1979–80	3	2	3	7	2	5	3
Total	22			13		24	
Five-year climatological percentage frequency of occurrence	11.2	13.8	7.5	11.0	4.2	25.2	11.5
Total	32.5			15.2		36.7	

ability. A ratio of the two variables is used because it is a measure of the liquid water available in a cloud to each natural ice crystal present. The LWC/ICC ratio is then the amount of liquid water available to each ice crystal if all the water in a given volume were equally distributed among the ice crystals present. A new ice crystal introduced into such an environment by seeding would have approximately that amount of water available for its growth.

For example, a cloud which exhibits a LWC/ICC of 10 μg per crystal has 10 μg of water available to each ice crystal for its growth, or 10 μg available for each new crystal that is introduced. The mass of ice crystals has been related to size by many investigators. According to Nakaya and Terrada (1935), a 10 μg plane dendrite has a diameter of about 1.5 mm and a 10 μg spatial dendrite has a diameter exceeding 1 mm. A 10 μg needle could exceed several millimeters in length. Therefore, if 10 μg of water in such a hypothetical cloud were available to each new ice crystal, they would grow to sufficient size to form precipitation.

If it were desired to significantly increase the ICC in a cloud by seeding, the liquid water available per crystal would have to be distributed over the total ICC which includes both the old and new crystals. For instance, if the ICC were to be doubled, a rough estimate of the water available to each new crystal would be half of the LWC/ICC ratio. Better estimates would consider the sizes and habits of the crystal population and stochastic processes.

The LWC/ICC ratio could be the same in a cloud that has a large LWC and a large ICC or in a cloud that has a small LWC and a small ICC. Such a measure of seedability, then, is not a measure of the amount of precipitation that would be expected from a cloud, but rather, a measure of the susceptibility of such a cloud to seeding.

A few difficulties are encountered when attempting to use the ratio of LWC to ICC. When no ice crystals are observed, the ratio is undefined. These instances accounted for less than 3% of the total number of in cloud observations. We have removed such cases from our samples because of the mathematical intractability of undefined quantities. In some of these cases the cloud was highly seedable with abundant LWC and no ice crystals. In others the cloud had little LWC, but again no ice crystals. These two separate conditions cannot be distinguished. A second problem in using the ratio is the minimum observable values of LWC and ICC. This problem would be no different in degree from considering the variables separately. However, the effect is distributed when a ratio is used rather than being fixed at a minimum cut-off value as it would be when considering a single variable.

5. Results of the climatological study of LWC and ICC in the central Sierra Nevada

This section presents the analysis of 98 h of aircraft data compiled over the 2-year period of study. The 98 h include 45 aircraft missions flown over 38 d. The number of missions flown in each year was nearly identical, with 23 missions included from the 1978–79 season and 22 missions from the 1979–80 season. The results are presented as relative frequency of occurrence which is defined as f/n, or percentage frequency as defined by $100\,f/n$, where f is the frequency of an event given n opportunities.

The data presented in the following subsections were collected "in cloud". "In cloud" is defined by an observation of droplet concentration greater than 10 cm^{-3} by the FSSP or an observation of ICC greater than 1 L^{-1} by the 2D-C.

a. Frequency in cloud

The in cloud percentages were greatest in area-wide echo types and least in cellular echoes (Fig. 4). These trends reflect the general environment in which each PET existed. The clouds defining area-wide echoes fill the sky with few breaks, though there may be cloud-free layers. Clouds associated with banded echo types often exist with clear sky ahead and behind the feature producing a lower percent in cloud frequency. However, the band is often associated with vigorous convection. Cellular clouds exhibit large areas of clear air between cells and in the valley and foothill region, thus providing the lowest percentage of being in cloud.

b. Distribution of LWC and ICC by temperature

This section presents the distribution of LWC, ICC, and the ratio of liquid water content over ice crystal concentration (LWC/ICC). The following figures show the percentage of time specific microphysical characteristics are observed normalized to in cloud observations made every 2.5°C.

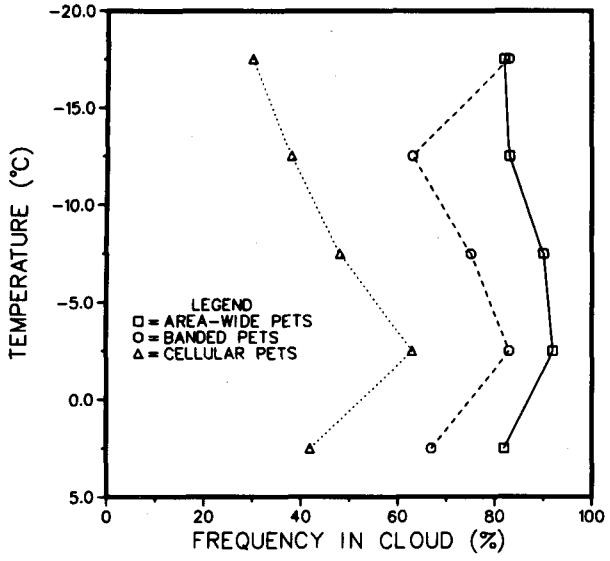

FIG. 4. Percentage of flight in cloud by temperature for area-wide, banded and cellular echo combinations.

The distributions of LWC, ICC, and the ratio of LWC/ICC are shown for the area-wide echo types in Figs. 5a–c, respectively. The LWC rarely exceeded 0.2 g m^{-3}. ICC in area-wide echo types was characterized by a narrow distribution of concentration from 10 to 100 L^{-1} and by little temperature variation. LWC/ICC ratios were found to be as large as 100 μg per crystal near the freezing level with a decline of ratios (to 10 μg per crystal) at lower temperatures. Ice crystals dominated liquid water, especially at temperatures less than −5°C.

The banded conditions, displayed in an analogous manner in Figs. 6a–c, are similar to those found in the area-wide episodes. Relatively less LWC was observed near the freezing level, though more LWC was found at temperatures less than −5°C. Liquid water contents > 0.25 g m^{-3} were found at temperatures from −5 to −15°C. Ice crystal concentrations were more broadly distributed than were those observed in the more stable echo types. Large concentrations, 100 to 1000 L^{-1}, were dominant at temperatures less than −5°C, whereas lower values, down to 1 L^{-1}, were found at greater temperatures. LWC/ICC ratios show virtually no difference from ratios observed in the area-wide echo environment.

Results for the cellular echo types are shown in Figs. 7a–c. Water contents were greater than those in the other two echoes discussed, with LWC above 0.5 g m^{-3} observed. The distribution of ICC was very broad with occurrences observed from 0.1 to nearly 1000 L^{-1}. Of perhaps most significance is the measurement of low ICC, a phenomenon virtually absent in the area-wide and banded echo types. The LWC/ICC ratios are more widely distributed with ratios above 100 μg per crystal frequently observed.

c. *Distribution of LWC and ICC in vertical cross section*

To formulate useful generalizations regarding the relationship between microphysical parameters and the terrain over which they are measured, relative frequency distributions of LWC, ICC, and LWC/ICC are presented in an east–west vertical plane roughly perpendicular to the Sierra crest. In orographically enhanced storm environments, specific orographic features can be distinguished by an increase of LWC. Some of these LWC maxima on the windward side of

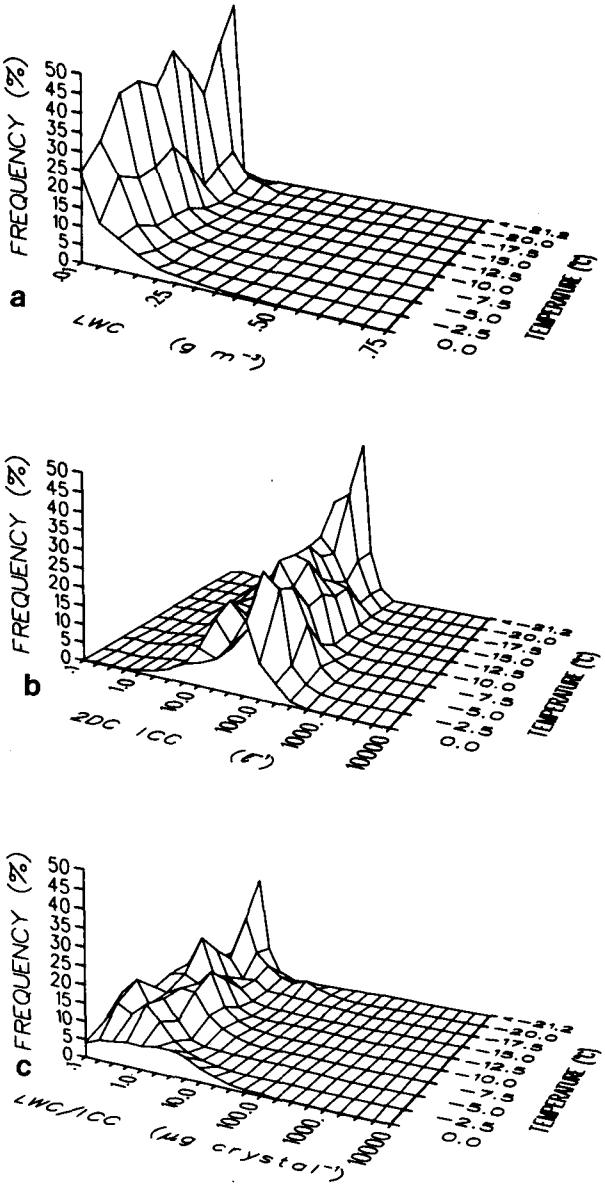

FIG. 5. (a) LWC distribution shown as a percentage of in cloud observations by 2.5°C temperature intervals for area-wide echo types; (b) same as (a) except ICC shown; (c) same as (a) except LWC/ICC shown.

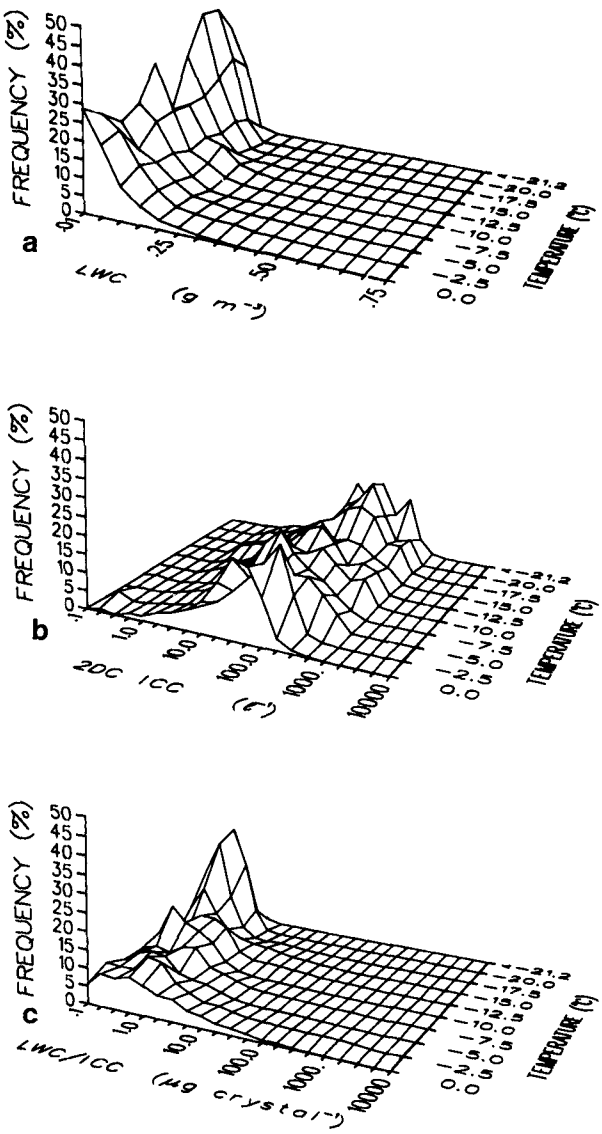

FIG. 6. (a) LWC distribution shown as a percentage of in cloud observations by 2.5°C temperature intervals for banded echo types; (b) same as (a) except ICC shown; (c) same as (a) except LWC/ICC shown.

mountain barriers have been shown by Hobbs (1975a,b), Marwitz (1980), and Lamb *et al.* (1976).

Figures 8–10 show the effect of the Sierra Nevada barrier on the cloud microphysics. The scribed boundaries delineate an area within which there were 100 or more in-cloud observations drawn from 10 km by 5°C grids. The Sierra mountain barrier projection, also shown in the following figures, was constructed by conversion of terrain elevations, averaged from 40 km north through 40 km south of a true east–west line from the SKYWATER radar, to temperatures taken from the standard atmosphere temperature-to-altitude relationship. Since temperatures were often less than those of the standard atmosphere, the data were usually closer to the crest projection than shown.

Examined here are the relative frequency of time the following microphysical conditions existed: 1) LWC exceeded 0.1 g m^{-3}, 2) ICC were less than 5 L^{-1}, and 3) LWC/ICC ratio exceeded 10 μg per crystal. These minimum conditions are believed to be necessary for seeding potential based on in cloud seeding experiments made in the Sierra and reported by Marwitz and Stewart (1980).

Figures 8a–c show the cloud microphysics cross sections for the area-wide echo types. Fig. 8a depicts a general absence of LWC greater than 0.1 g m^{-3}, but

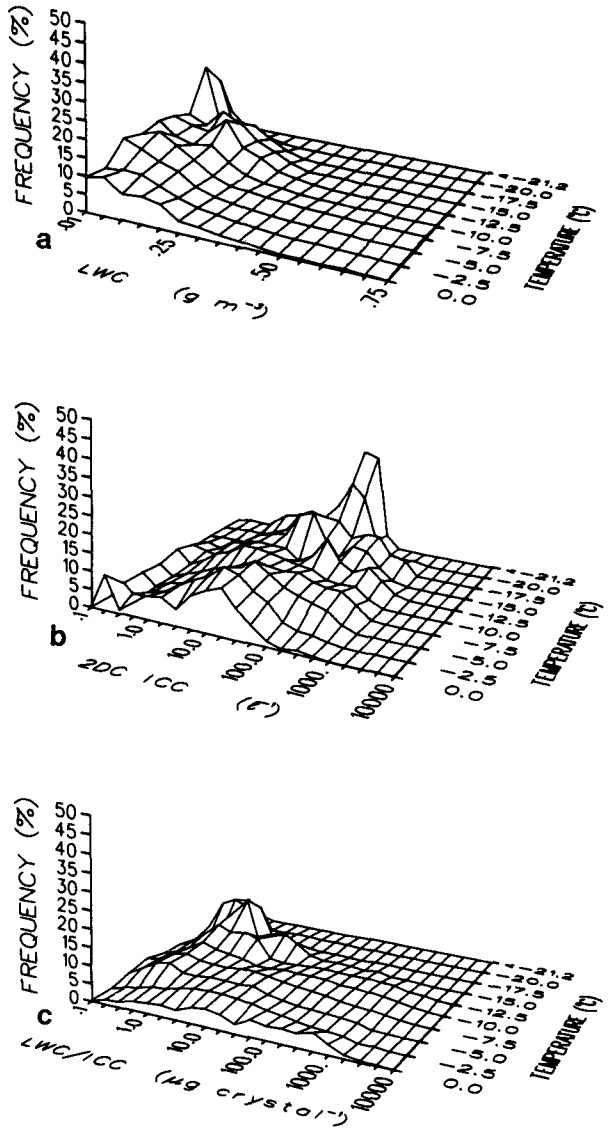

FIG. 7. (a) LWC distribution shown as a percentage of in cloud observations by 2.5°C temperature intervals for cellular echo types; (b) same as (a) except ICC shown; (c) same as (a) except LWC/ICC shown.

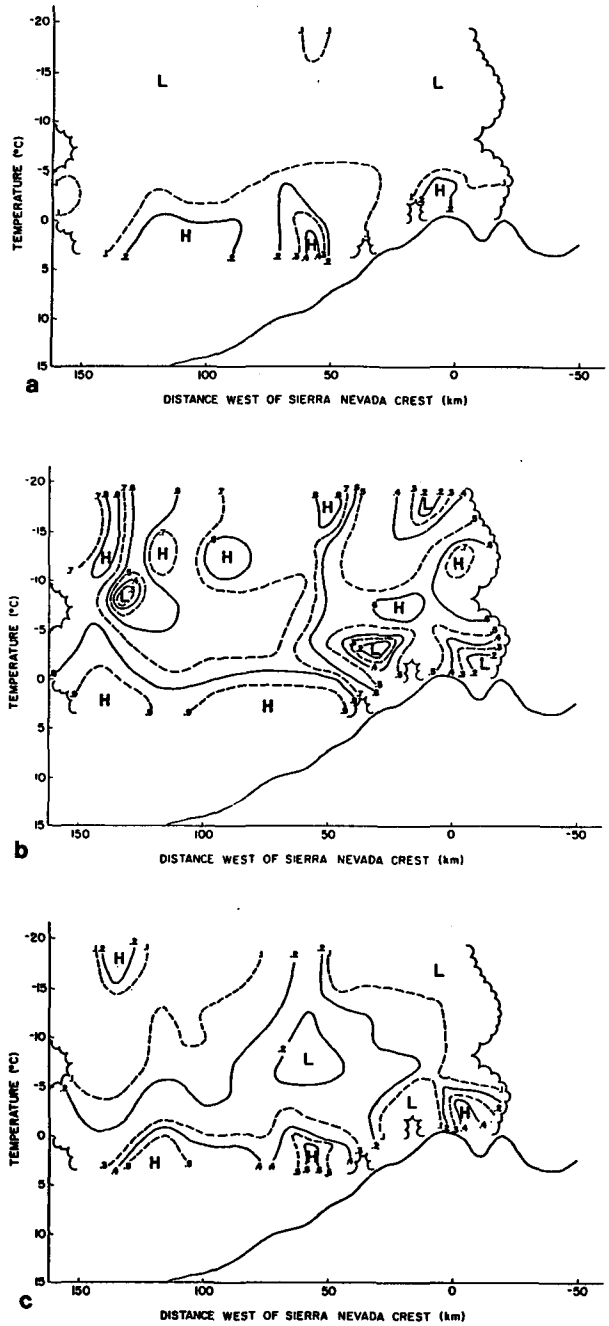

FIG. 8. (a) Distribution of LWC > 0.1 g m^{-3} shown in cross section as a relative frequency of in cloud observations tabulated for 10 km by 5°C grids for area-wide echo types. Cloud markings indicate an area within which 100 in cloud observations were made; (b) same as (a) except ICC < 5 L^{-1} shown; (c) same as (a) except LWC/ICC > 10 μg per crystal shown.

the relative frequencies were greater near the freezing level and there was a dramatic decrease with lower temperatures. The relative frequency of ICC < 5 L^{-1} was a maximum near the freezing level. Frequencies decreased, ICC increased, closer to the crest and with lower temperatures (Fig. 8b). Measurements of LWC/ICC > 10 μg per crystal were rarely observed in the area-wide combination. More substantial relative frequencies (>0.5) occurred in pockets near the freezing level 40 to 120 km upwind of the Sierra barrier (see Fig. 8c).

Figures 9a–c show the cloud microphysics cross sections for banded echo types. Greater relative frequen-

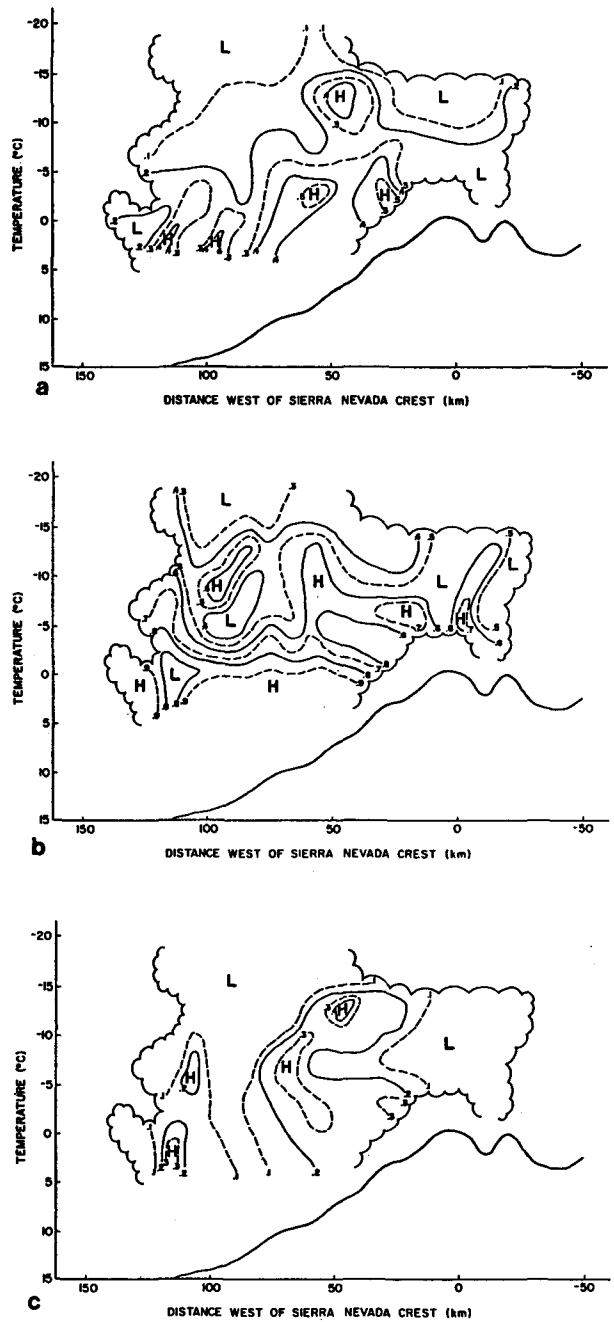

FIG. 9. (a) As in Fig. 8a, but for banded echo types; (b) same as (a) except ICC < 5 L^{-1} shown; (c) same as (a) except LWC/ICC > 10 μg per crystal shown.

cies of liquid water were observed than in the area-wide conditions. LWC of 0.1 g m^{-3} or greater were observed 40% of the time up to −15°C 50 km west of the crest. A secondary maximum is evident 120 km west of the crest. Fig. 9b shows the ICC stratification characteristics for the banded cases. A region of low ICC relative frequencies was found in the higher temperatures, though in regimes less than −5°C there was nearly a 50/50 chance of these conditions being met. The ratio of LWC/ICC, shown in Fig. 9c, showed the largest relative frequencies in the high temperatures, similar to the area-wide cases, with smaller values at temperatures less than −5°C.

Within cellular echo types LWC > 0.1 g m^{-3} was measured over a broad expanse from 40 to 90 km west of the crest (Figs. 10a–c). These conditions were observed 50% of the time from 0°C through −15°C. This figure is most useful in showing where convective supercooled liquid water clouds generally form on the mountain barrier, as indicated by the strong horizontal gradient 90 to 100 km west of the crest. In the general area where LWC relative frequencies were greatest, the relative frequencies of low ICC appears to be maximized. The relative frequency of ratios confirm this coincidence. LWC/ICC ratios > 10 μg per crystal were observed 60% of the time at distances 40 to 100 km west of the Sierra crest, with a secondary maximum evident directly above the crest.

d. Extent of significant liquid water regions

The extents of regions having significant LWC were evaluated by determining the distance flown in cloud while within significant LWC. A threshold of 0.2 g m^{-3} was used as a measure of significance, two temperature regions ($0 > T \geq -10$°C, $T < -10$°C) were considered, and data were stratified by PET. If the 0.2 g m^{-3} criterion was not satisfied within a small pocket (<1 km) but was satisfied within adjacent regions, the calculated extent of the region ignored the pocket.

Figures 11a and 11b show the relative frequency that regions containing significant LWC were encountered at $0 > T \geq -10$°C and $T < -10$°C, respectively. At the higher temperatures, regions 32–64 km wide occurred in all PET categories, but the relative frequency of significant LWC regions, regardless of extent, was greatest for cellular echoes and least for area-wide echoes. At the lower temperature, cellular echoes contained the widest regions of significant LWC (up to 32 km), whereas the regions of significant LWC in area-wide echoes were only 2–4 km wide. Furthermore, the frequencies of LWC regions were similar in the cellular and banded echoes up to 8 km, but no regions wider than this occurred in the banded echoes.

A comparison of characteristics between the two temperature regimes reveals distinct differences. In particular, regions containing significant LWC were wider at the higher temperatures in all PET categories. Relative frequencies generally were greater at the higher temperatures, except for banded echoes < 8 km in width in which case the frequencies at the two temperature regimes were similar.

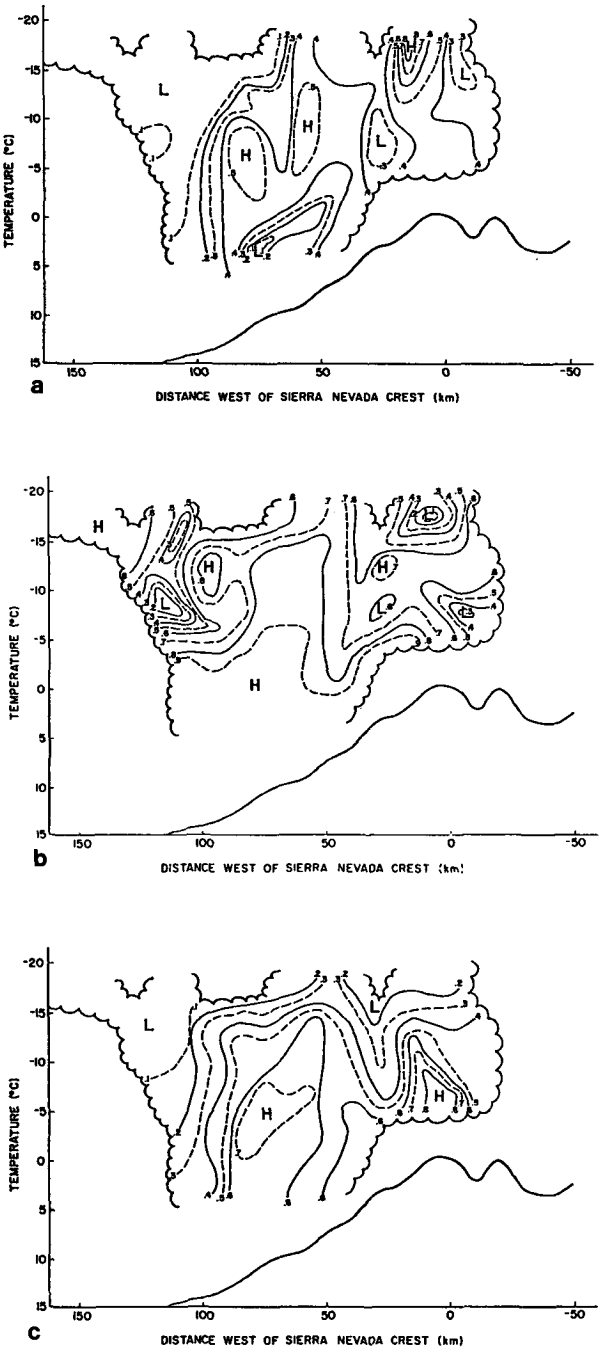

FIG. 10. (a) As in Fig. 8a, but for cellular echo types. Cloud markings indicate an area within which 100 in cloud observations were made; (b) same as (a) except ICC < 5 L^{-1} shown; (c) same as (a) except LWC/ICC > 10 μg per crystal shown.

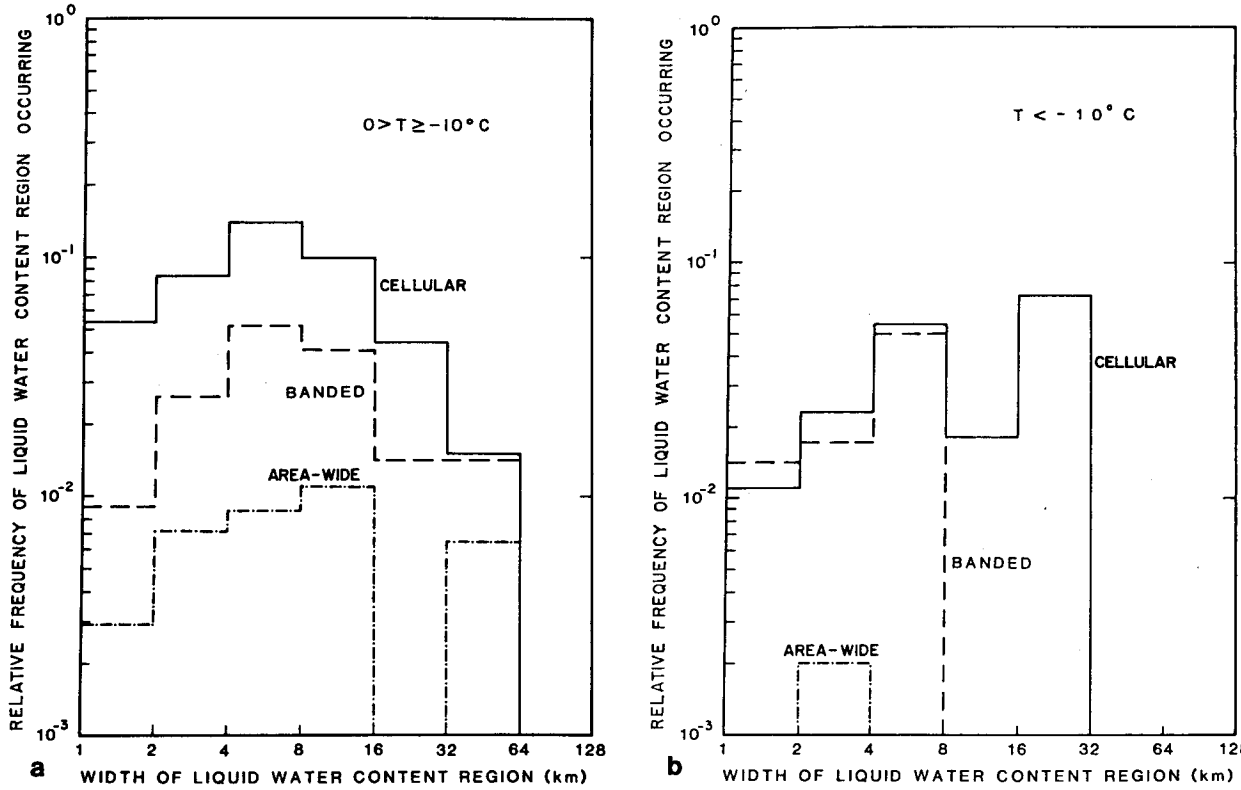

FIG. 11. (a) Distribution of the extent of regions of cloud where LWC > 0.2 g m^{-3} at temperatures from 0 to −10°C shown for the area-wide, banded and cellular echo combinations; (b) same as in (a) except temperatures less than −10°C shown.

e. Stratification by 700 mb trough passage

This section examines the relationship between the relative frequency of LWC/ICC ratios > 10 μg per crystal and the 700 mb trough environment. Both Hobbs (1975a,b) and Lamb *et al.* (1976) have alluded to a relationship between the occurrence of high LWC and the postfrontal air mass. The results of this analysis not only reveal this relationship, but also a certain time dependency. The 700 mb trough position was obtained from time section analyses of rawinsonde data.

Figure 12 shows the relative frequency that LWC exceeded 10 μg per crystal by observation temperature in the post-trough environment. Maximum relative frequencies of large LWC/ICC ratios usually did not exceed 0.2 in the pretrough observations. The relative frequency that LWC/ICC ratios exceeding 10 μg per crystal were observed did not exceed 0.2 until 7 h after 700 mb trough passage. Recall that the occurrence of the C1 PET peaked at this same time. The relative frequency maximum is sloped from a temperature of approximately −15°C at 7 h after passage to 0°C, 9 h after trough passage. This may indicate deteriorating convective conditions with time, resulting in shallower clouds with warmer tops. Beyond 10 h after trough passage relative frequencies dropped below 0.2. The optimum time that large relative frequencies were encountered ranged from 7 to 10 h after 700 mb trough passage.

6. Conclusions

The results have provided a close look at the supercooled LWC and ICC in winter storms of the central Sierra Nevada for the two successive years, 1978–80. It should be mentioned that minimum observed clearance altitude restrictions prevented the aircraft from flying within ~1 km of the Sierra terrain, and it is possible that large LWC exist in this layer.

The cellular echo types clearly exhibit the most desirable characteristics of significant liquid water and relatively little ice. The extent of this region is bounded in the vertical by the 0 to −15°C isotherms and its core 40 to 100 km upwind of the crest. The horizontal extent of significant LWC was also greatest within the cellular PET, with segments 32 to 64 km wide frequently measured.

The area-wide and banded echo types provide fewer instances of significant supercooled water and absence of ice. LWC were strictly confined to the higher tem-

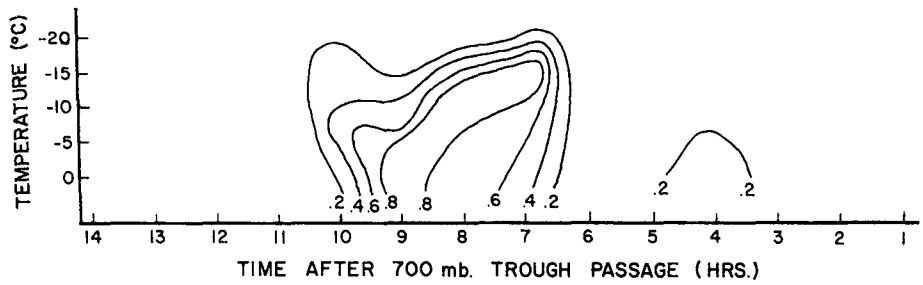

FIG. 12. Distribution of LWC/ICC > 10 μg per crystal shown in time section as a relative frequency of in cloud observations relative to the 700 mb trough passage time.

perature zones, 0 to −5°C whereas ice crystals generally dominated the cloud physics at lower temperatures. In particular echoes were typically associated with ice crystal concentrations up to an order of magnitude greater than concentrations observed in area-wide and cellular echo types at temperatures less than −5°C.

Liquid water maxima were found near the freezing level irrespective of PET. This translated to a LWC/ICC ratio > 10 μg per crystal, having more than a 50% observation frequency at temperatures around 0°C for all three echo combinations. LWC maxima were generally found 40–120 km west of the crest; beyond 120 km, effects of the mountain are unnoticeable. The release of convective instability or the forced lifting of the airmass over the barrier starts to introduce increasing amounts of LWC which are rapidly transported to supercooled environs. Between 40 and 120 km west of the crest, ice crystals begin to form and grow at the expense of the LWC. As the precipitation process continues, ice crystal multiplication probably becomes a dominant factor, causing a large decrease in LWC/ICC ratios as the air moves closer to the crest. The barrier at 40 km roughly intersects the freezing level on average storm days, so that east of this region the introduction of additional liquid water by convection is limited. The depletion of the liquid water by accretion also probably lowers LWC/ICC ratios at distances closer than 40 km to the crest.

Large relative frequencies of LWC/ICC > 10 μg per crystal were well displaced from the time of the 700 mb trough passage. These were first noticeable 6 h after the trough passage, with the largest relative frequencies found 7 to 10 h after the 700 mb trough passage. The available vertical depth for convection, bounded below by the ground and above by the front, appears to be an extremely important feature for the growth of clouds.

The general conclusions reached in this study agree with previous work conducted on west coast orographic storms. Hobbs (1975a,b) found that ice particles dominate over liquid water in prefrontal conditions in storms over the Cascade Mountains of Washington State, and also found that ratios of ice to water were less in postfrontal segments than prefrontal segments of storms. The findings in the Sierra Nevada closely follow the findings of Hobbs. As well, Lamb *et al.*, (1976) showed in Sierra storms that microphysical seeding opportunities were generally related to intense convection and that the greatest amounts of LWC were found 40–75 km upwind and to the west of the Sierra Nevada crest. Our findings concur with those of Lamb *et al.*

This research has determined from aircraft observations the distribution of water and ice within Sierra Nevada winter storms. It is evident that these properties are dependent upon storm conditions. Nevertheless, the information clearly indicates that the cellular cloud type represents, at least from the microphysical viewpoint, the best candidate for a snowfall enhancement project. The SCPP has used these results in part to design SCPP-1, a randomized CO_2 experiment on the cellular PET.

Acknowledgments. The authors wish to thank the many participants of the SCPP who made this study possible. Particular thanks are given to the University of Wyoming, Department of Atmospheric Science for collecting the aircraft data and providing comments. The concept of LWC/ICC ratio was partially developed during discussions with Dr. John Marwitz. The authors appreciate the diligence exhibited by the typist J. Dutton and the drafting which was done by K. Dreher.

REFERENCES

Cooper, W. A., 1978: Cloud physics investigations by the University of Wyoming in HIPLEX 1977. Dept. of Atmos. Sci., University of Wyoming, 320 pp.

——, and J. D. Marwitz, 1980: Winter storms over the San Juan Mountains. Part III: Seeding potential. *J. Appl. Meteor.*, **19**, 100–107.

——, and C. P. R. Saunders, 1980: Winter storms over the San Juan Mountains. Part II: Microphysical processes. *J. Appl. Meteor.*, **19**, 927–941.

Hobbs, P. V., 1975a: The nature of winter clouds and precipitation in the Cascade Mountains and their modification by artificial seeding. Part I: Natural conditions. *J. Appl. Meteor.*, **14**, 783–804.

——, 1975b: The nature of winter clouds and precipitation in the Cascade Mountains and their modification by artificial seeding.

Part III: Case studies of the effects of seeding. *J. Appl. Meteor.*, **14,** 819–858.

——, and L. R. Radke, 1975: The nature of winter clouds and precipitation in the Cascade Mountains and their modification by artificial seeding. Part II: Techniques for the physical evaluation of seeding. *J. Appl. Meteor.*, **14,** 805–818.

Knollenberg, R. G., 1972: Comparative liquid water content measurements of conventional instruments with an optical array spectrometer. *J. Appl. Meteor.*, **11,** 501–508.

——, 1976: Three new instruments for cloud physics measurements. The 2-D spectrometer, the forward scattering spectrometer probe, and the active scattering aerosol spectrometer. *Preprints Int. Conf. Cloud Physics,* Boulder, CO, Amer. Meteor. Soc., 554–561.

Lamb, D., K. W. Nielsen, H. E. Klieforth and J. Hallet, 1976: Measurement of liquid water content in winter cloud systems over the Sierra Nevada. *J. Appl. Meteor.*, **15,** 763–775.

Marwitz, J. D., 1980: Winter storms over the San Juan Mountains, Part V: Dynamical processes. *J. Appl. Meteor.*, **19,** 913–926.

——, and R. E. Stewart, 1978: Cloud physics studies in Utah during 1978. Rep. No. AS 122, Dept. of Atmos. Sci., University of Wyoming, 3–8.

——, and ——, 1981: Some seeding signatures in Sierra storms. *J. Appl. Meteor.*, **20,** 1129–1144.

Nakaya, V., and T. Terada, 1935: Simultaneous observations of the mass, falling velocity, and form of individual ice crystals. *J. Fac. Sci. Hokkaido Univ., Ser. II,* **1,** 191.

Schroeder, M. J., and G. E. Klazura, 1978: Computer processing of digital radar data gathered during HIPLEX. *J. Appl. Meteor.*, **17,** 498–507.

Strapp, J. W., and R. S. Schemenauer, 1982: Calibrations of Johnson-Williams liquid water content meters in a high-speed icing tunnel. *J. Appl. Meteor.*, **21,** 98–108.